Journal of Engineering Science and Technology
24th EURECA 2025 Special Issue April (2026) 1 - 15

MWCNTS-PNIPAAM THERMORESPONSIVE MEMBRANE FOR KITCHEN WASTEWATER TREATMENT: EFFECT OF MWCNTS DIAMETER

AYMAN NABIL ALADIN @ MOHD NAZRI[1], KAH CHUN HO[1,2,3,*], JIUN HOR LOW[1,2,3], JIA LEANG TEH[1], YEIT HAAN TEOW[4]

[1]School of Engineering, Faculty of Innovation and Technology, Taylor's University, No. 1, Jalan Taylor's, 47500 Subang Jaya, Selangor, Malaysia.
[2]Clean Technology Impact Lab, Taylor's University, No.1, Jalan Taylor's, 47500 Subang Jaya, Selangor, Malaysia
[3]Centre for Sustainable Societies, Taylor's University, No.1, Jalan Taylor's, 47500 Subang Jaya, Selangor, Malaysia
[4]Department of Chemical and Process Engineering, Faculty of Engineering and Built Environment, Universiti Kebangsaan Malaysia, 43600 UKM Bangi, Selangor Darul Ehsan, Malaysia
*Corresponding Author: kahchun.ho@taylors.edu.my

Abstract

Kitchen wastewater (KWW) poses significant challenges to water quality. Membrane filtration has emerged as a promising solution, though membrane fouling remains a major limitation. This study aimed to investigate the effects of multi-walled carbon nanotubes (MWCNTs) diameters (12-15 nm, 20-30 nm) in MWCNTs-poly(N-isopropylacrylamide) (PNIPAAm) for enhanced membrane characteristics and performance in the treatment of KWW. This is evident as MWCNTs-PNIPAAm membranes with larger MWCNTs diameter showed high permeability (25.08 $L/m^2 \cdot h \cdot bar$) and consistent high SOW rejections (98.82% and 85.60%). Overall membrane performance was governed by structural and surface property modifications, where increased porosity, pore size, and hydrophilicity enhanced membrane permeability, while SOW rejection was influenced by the corresponding pore structure. Ultimately, the membrane found to be the optimal was membrane blended by MWCNTs-PNIPAAm with smaller MWCNTs diameter. This is due to its high permeability (23.10 $L/m^2 \cdot h \cdot bar$), its attainment of the highest values of normalized flux (0.736 and 0.774) and FRR (0.876), as well as stable SOW rejections (68.45% and 69.30%). The testing with actual KWW resulted in high rejections of COD (≈84%), total suspended solids (TSS ≈ 84%), and colour (89%), with the pH closer to neutral value. Comparisons with the National Water Quality Standards of Malaysia (NWQSM) confirmed that the Class IV limits have been met, making the effluent KWW suitable for the reuse in non-potable activities.

Keywords: Kitchen wastewater, Multi-walled carbon nanotubes (MWCNTs), Poly(N-isopropylacrylamide), (PNIPAAm)Thermoresponsive membrane.

1. Introduction

Kitchen wastewater (KWW) is defined as effluent water free of human urine or faeces that are sourced from kitchen sinks [1]. The generation of KWW primarily comes from households, restaurants, and food processing facilities, particularly from cooking, cleaning, and washing [2]. Their composition can largely vary due to the mixture of organic and inorganic substances that is influenced by the dietary preferences and cooking habits. KWW components consist of starchy residues, plant fibres, animal fats, and proteins, as well as surfactants from detergents and soaps [1, 3].

Therefore, KWW generally contains elevated concentrations of chemical oxygen demand (COD), biochemical oxygen demand (BOD), fats, oil, and grease, nutrients, and heavy metals [2, 3]. If not properly treated, the release of these pollutants will play a significant role in the degradation water bodies, damage on infrastructures and pose risks towards both humans and the environment [1]. The complexity and inconsistency of the KWW characteristics have made it difficult to remove all contaminants effectively.

Membrane separation has gained significant popularity as a wastewater treatment method due to many advantages including low energy requirement, compact system, and capability in producing high water quality. However, membrane fouling remains as the major drawback as it reduces the membrane's water flux and overall separation performance. To overcome this issue, the incorporation of nanoparticles into the membrane matrix has been widely explored to minimize the effects of fouling [4]. One of the nanomaterials that has garnered significant attention is multi-walled carbon nanotubes (MWCNTs) because of their large specific surface area, unique pore structure, and high mechanical and thermal strength [5].

Nonetheless, these enhancements are still unable to fully combat membrane fouling over long period use. Therefore, membrane cleaning or replacements are still required regularly, which in turn contributes to higher operational costs. A recent advancement made in membrane technology is the discovery of smart polymers. Poly(N-isopropylacrylamide) (PNIPAAm) is a thermoresponsive polymer that is able to swell and shrink when the surrounding temperature changes between its lower critical solution temperature (LCST) of around 32 °C [4, 6]. From this, the integration of an active temperature sensitive cleaning mechanism can provide an effective strong washing force for foulant removal [5].

MWCNTs and PNIPAAm possess individual advantageous properties that make them attractive for advanced membrane development. Despite this, the use of MWCNT-PNIPAAm thermoresponsive membranes for KWW treatment remains underexplored. Most existing research focuses on biomedical applications, particularly tissue engineering, due to the biocompatibility and electrical conductivity possessed by the nanocomposite [7]. In the field of wastewater treatment, only a limited number of related studies have been reported. This includes the treatment of dairy wastewater using MWCNTs-PNIPAAm [5] and the application of silica (SiO_2)-PNIPAAm for saline oil emulsion treatment [4].

Both studies investigated different concentrations of thermoresponsive nanocomposites within the membrane matrix. However, there is still very limited research conducted on MWCNTs-PNIPAAm membranes for treating KWW, in which varying MWCNTs diameters are evaluated. The structure of MWCNTs significantly affects how the thermoresponsive nanocomposite is distributed within

the membrane matrix, resulting in strong washing that effectively remove foulants through alternating temperatures. Therefore, the aim of this study is to determine the optimal diameter of MWCNTs (12-15 nm, 20-30 nm) in MWCNTs-PNIPAAm membrane that can provide a straightforward and environmentally friendly process that supports the potential reuse of treated KWW.

2. Materials and Methods

2.1. Materials

MWCNTs with two different diameters (12-15 nm, 20- 30 nm) and purity greater than 97% were supplied by Ugent Tech, Malaysia and NanoAmor, USA, respectively. Nitric acid was obtained from Chemiz, Malaysia. Ethanol (99.9%) was obtained from J.T. Baker, USA, while acetic acid (99.85%) was obtained from Bendosen, Malaysia. 3-methacryloxypropyltrimethoxysilane (MPS) with purity 98%, N-isopropyl acrylamide (NIPAAm) with purity 97% and N,N-methylene bisacrylamide (MBA) with purity 98% were obtained from Macklin, China. Potassium persulfate (KPS) with purity 99%, dimethylacetamide (DMAc) with purity 99.9% and sodium dodecylbenzenesulfonate (SDBS) were obtained from Sigma-Aldrich, USA. Hydrogen peroxide (30%) was obtained from Systerm, Malaysia, while polyvinylidene fluoride (PVDF) was obtained from Shanghai Ofluorine Co., China. Vegetable oil was obtained from Buruh, Malaysia.

2.2. Synthesis of MWCNTs-PNIPAAm thermoresponsive membrane

2.2.1. Oxidation of MWCNTs

First, 0.2 g of MWCNTs was added to 70 mL of 3 M nitric acid [5, 8]. The mixture was then placed on a magnetic stirrer and stirred at 60 °C for 15 minutes. Subsequently, the mixture was sonicated in an ultrasonic bath (Elmasonic P, Elma, Germany) at 80 W and 37 kHz for 2 hours to enhance dispersion and promote surface oxidation. Afterward, the residual nitric acid was removed via centrifugation, and the MWCNTs was repeatedly rinsed with deionized (DI) water until neutral pH was reached. Next, the washed MWCNTs was introduced to 70 mL of 30% hydrogen peroxide under the same stirring and sonification conditions. Once the second oxidation was complete, the MWCNTs was washed again to neutrality and finally freeze-dried at -100 °C for 24 hours.

2.2.2. Silanization of MWCNTs

The silanization of MWCNTs was carried out via silane hydrolysis [5, 7]. An 80 mL mixture consisting of ethanol and distilled water at a volumetric ratio of 80:20 was prepared. Following this, the pH of the mixture was adjusted to the range of 3.5 to 4.5 by the addition of acetic acid. Then, 0.4 g of MPS was added to the mixture, followed by uniform dispersion using an ultrasonic bath (Elmasonic P, Elma, Germany) operating at 80 W and 37 kHz for an hour.

The mixture was subsequently heated and continuously stirred on a hot plate at 60 °C for 4 hours. The resulting ethanol-water mixture was separated through centrifugation. Finally, the silanized MWCNTs were washed three times with DI water and acetone in sequence, then freeze-dried for 24 hours at -100 °C using a freeze dryer.

2.2.3. Radical polymerization

Initially, 120 mL of a solvent mixture consisting of DMAc and DI water in a 1:1 volume ratio was prepared [4, 5]. Subsequently, 0.5 g of NIPAAm and 0.03 g of MBA, along with 0.2 of the previously silanized MWCNTs, was added to the mixture. The mixture was then sonicated in an ultrasonic bath (Elmasonic P, Elma, Germany) at 80 W and 37 kHz for 30 minutes to ensure uniform dispersion. After sonication, the mixture was purged with nitrogen gas and stirred overnight at 70 °C under a nitrogen atmosphere using a magnetic hot plate.

Following this initial mixing, 0.02 g of KPS was introduced as the initiating agent. The mixture was again purged with nitrogen and maintained under identical conditions, with continuous stirring at 70 °C overnight to complete the polymerization process. Upon completion of reaction, the supernatant was removed by centrifugation, and the product was washed three times with DI water. Finally, the product was freeze-dried at -100 °C for 24 hours to obtain the produced MWCNTs-PNIPAAm nanocomposite.

2.2.4. Preparation of MWCNTs-PNIPAAm thermoresponsive membrane

The thermoresponsive membranes incorporating the MWCNTs-PNIPAAm nanocomposite were prepared via the immersion precipitation phase inversion [5]. Initially, the required mass of MWCNTs-PNIPAAm nanocomposite (with respect to casting solution) was dispersed in 20.5 g of DMAc by sonication for 30 minutes in an ultrasonic bath (Elmasonic P, Elma, Germany) operating at 80 W and 37 kHz (Table 1). After uniform dispersion was achieved, 4.5 g of dried PVDF was introduced to the mixture, which was then stirred at 65 °C on a magnetic hot plate for 4 hours to prepare the casting solution.

The stirring continued for an additional 4 hours at room temperature. To eliminate entrapped air, the solution was stored in a desiccator overnight. The prepared solution was subsequently cast on a membrane support (CU414 Opti, Neenah US) taped onto a clean glass plate to achieve a thickness of 200 μm. Upon completion of casting, the plate was immediately immersed in a tray containing 5 L of distilled water and left overnight to allow polymer precipitation and formation of asymmetric porous membranes. Pristine MWCNTs were used as controlled membranes.

Table 1. Composition of membranes.

Membrane	MWCNTs diameter (nm)	MWCNTs (wt%)	MWCNTs-PNIPAAm nanocomposite (wt%)
M0	-	-	-
M1a	12 - 15	0.05	-
M1b	12 - 15	-	0.05
M2a	20 - 30	0.05	-
M2b	20 - 30	-	0.05

2.3. Membrane and nanocomposite characterization

2.3.1. Membrane morphology

The morphology of the membranes was analysed using a Scanning Electron Microscope (SEM) (Hitachi TM3000, Tokyo, Japan) at magnification of 1 k ×. and

15.0 kV. For cross-sectional imaging, the membranes were immersed in liquid nitrogen and fractured to produce a clean cross-sectional view. For top surface imaging, the membranes were cut into 0.5 cm × 0.5 cm pieces and observed directly.

2.3.2. Porosity and pore size

Membrane porosity was calculated using the gravimetric method. The membrane samples were first immersed in distilled water for 12 hours and then cut into 1 cm × 1 cm pieces. After that, excess water on the surface of the membrane was gently removed with filter paper prior to weighing. The samples were subsequently dried at 50 °C for 24 hours and weighed again. The measurements of the thickness of the membranes were obtained using a digital micrometre. Porosity values were then determined according to Eq. (1) [9].

$$\varepsilon = \frac{w_2 - w_1}{A \times l \times d_w} \quad (1)$$

where ε is membrane porosity, w_1 is dry membrane mass (g), w_2 is wet membrane mass (g), A is membrane surface area (m^2), d_w is density of water (kg/m^3) and l is thickness of membrane (m).

Based on the calculated porosity, the Guerout-Elford-Ferry equation (Eq. 2) [3] was used to determine the mean pore radius (r_m) of each membrane.

$$r_m = \sqrt{\frac{(2.90 - 1.75\varepsilon)8V\mu\delta}{\varepsilon PA}} \quad (2)$$

where r_m is mean pore radius of membrane (m), ε is porosity of membrane, V is volumetric flow rate of water (m^3/s), μ is dynamic viscosity of water at 25 °C (Pa·s), δ is thickness of membrane (m), P is applied pressure (Pa) and A is surface area of membrane (m^2).

2.3.3. Hydrophilicity

The hydrophilicity of the membrane surface was determined using a contact-angle meter (OCA 15EC, Dataphysics Instruments, Germany) to determine the water contact angle (WCA). The membrane was first secured onto a glass slide using double-sided tape, after which a 1 µL water droplet was deposited on the membrane surface. The resulting WCA was recorded with the high-speed camera of the instrument and then processed with dpiMAX software. To minimize experimental error, measurements were taken at three separate locations of each membrane [9].

2.4. KWW characterization

The kitchen wastewater was obtained from the School of Culinary, Taylor's University Malaysia. To preserve the kitchen wastewater, the wastewater was kept at 4 °C.

Characteristics of KWW including COD, total suspended solids (TSS), and colour was analysed using ultraviolet-visible (UV-Vis) spectrophotometer (Spectroquant Prove 300, Merck, Germany); while total dissolved solid (TDS) was measured using TDS meter (TDS & EC Meter, LIKDAY Instruments, China) and pH was analysed using a calibrated pH meter (pH 211, Hanna Instruments, USA) [10].

2.5. Membrane performance

The performance of the synthesized MWCNT-PNIPAAm thermoresponsive membranes was carried out using a custom-built bench-scale crossflow system with a 10 L capacity. The membrane samples were prepared as 4.7 cm diameter circular discs providing an effective filtration area of 17.3 cm^2 [10].

2.5.1. Membrane permeability

The membrane filtration process began with a pre-compaction step, where the membrane was filtered with distilled water for 30 minutes at a fixed transmembrane pressure (TMP) of 3 bar. This step stabilized the structure of the membrane and ensured steady flux measurements during the experiments [8].

Next, the permeability of the membrane was evaluated by conducting another filtration run using distilled water as the feed, with the TMP varied sequentially at 1.0, 1.5 and 2.0 bar, with each pressure maintained for 10 minutes. The mass of permeate was recorded at 1-minute intervals, and the corresponding permeate flux (J) was calculated using Eq. (3). A graph of permeate flux against TMP was then plotted, where the gradient of the resulting linear trendline was taken as the membrane permeability.

$$J = \frac{\Delta V}{A \Delta t} \tag{3}$$

where J is permeating flux (L/m·h), ΔV is volume of permeate (L), A is effective filtration area of membrane (m^2) and Δt is permeation time (h).

2.5.2. Normalized flux

SOW was prepared by mixing vegetable oil and distilled water at a fixed concentration, using SDBS as a surfactant, and sonicating for 15 minutes to obtain a stable emulsion. The fouling behaviour of the membrane was evaluated by calculating the normalized flux, shown in Eq. (4). The normalized flux was determined through two filtration runs. In the first run, 2 L of SOW was used as the feed, and the permeate mass was collected over 30 minutes at 1-minute intervals under a TMP of 2 bar.

Prior to the second run, the contaminated membrane was subjected to a cleaning process using an alternating thermal method. The cleaning done by passing distilled water at 40 °C and 25 °C (representing temperatures higher and lower than the PNIPAAm LCST, respectively), for 10 minutes at each temperature [4]. The second filtration run was then conducted using 2 L of SOW under the same operating conditions as the first run.

$$Normalized\ Flux = \frac{J_P}{J_W} \tag{4}$$

where J_P is permeating flux of SOW (L/m·h) and J_W is pure water flux (L/m·h).

The permeate flux obtained from prior filtration run using distilled water with the same membrane at 2 bar was used as the pure water flux (J_W), while the permeate flux from the two SOW filtration runs was considered as the permeate flux of SOW (J_P) [8].

2.5.3. Flux recovery ratio (FRR)

The efficiency of the cleaning process on the contaminated membrane can be used to evaluate the antifouling properties of the MWCNTs-PNIPAAm thermoresponsive membrane. To assess the efficiency of foulant removal, the flux recovery ratio (FRR) was determined using Eq. (5), as shown below.

$$FRR = \left(\frac{J_C}{J_W}\right) \times 100\% \quad (5)$$

where J_C is permeating flux after cleaning (L/m·h), J_W is permeating flux before cleaning (L/m·h).

2.5.4. Membrane rejection

After the filtration process, the collected permeate was analysed to assess the oil concentration of the treated SOW. For each water quality parameter, the rejection efficiency was calculated using Eq. (6) to quantify the overall performance of the membrane in improving effluent quality.

$$R = \left(1 - \frac{C_P}{C_F}\right) \times 100\% \quad (6)$$

where R is membrane rejection (%), C_P is permeating solution concentration, C_F is feed solution concentration.

For the filtration run treating actual KWW, the treated water characteristics were compared to the National Water Quality Standards of Malaysia (NWQSM) to verify compliance of treated water with regulatory requirements for discharge or reuse [11].

3. Results and Discussion

3.1. Membrane characterization

Table 2 shows the measured porosity and pore size of the prepared membrane. The measured pore sizes ranged from 15.71 to 20.27 nm, which falls within the typical range of 2 to 100 nm for ultrafiltration membranes [12]. In general, the porosity and pore size of the membranes increased upon the incorporation of MWCNTs nanoparticles (M1a and M2a) and MWCNTs-PNIPAAm nanocomposites (M1b and M2b) compared to the unmodified PVDF membrane (M0). The increased pore size by MWCNTs-PNIPAAm nanocomposites is attributed to the accelerated exchange between the solvent in the casting solution and the nonsolvent in the coagulation bath during phase inversion process. The presence of MWCNTs-PNIPAAm enhances solvent outflow and water influx. This promotes rapid liquid-liquid demixing which ultimately result in larger membrane pore formation [10, 13].

Table 2. Porosity and pore size of the prepared membranes.

Membrane	Porosity (%)	Pore size (nm)
M0	23.45 ± 2.01	17.38 ± 0.49
M1a	38.06 ± 0.85	15.71 ± 0.30
M1b	37.03 ± 1.76	18.12 ± 0.67
M2a	28.27 ± 3.34	17.92 ± 1.64
M2b	14.59 ± 1.05	20.27 ± 0.29

In addition, membranes prepared with smaller diameter MWCNTs of the same nanofiller exhibit higher porosity (M1a: 38.06% > M2a: 28.27% and M1b: 37.03% > M2b: 14.59%) due to the uniform dispersion which forms a stronger network that increase the membrane porosity [14]. However, larger diameter MWCNTs tend to agglomerate that weakens the reinforcing network in the polymer matrix [15]. This trend is also supported by the SEM images of the top surface (Fig. 1), where M1a (Fig. 1(a)) appears more porous than M1b (Fig. 1(b)), but is less porous than M2b (Fig. 1(c)), as indicated by the density of dark spots on the surface.

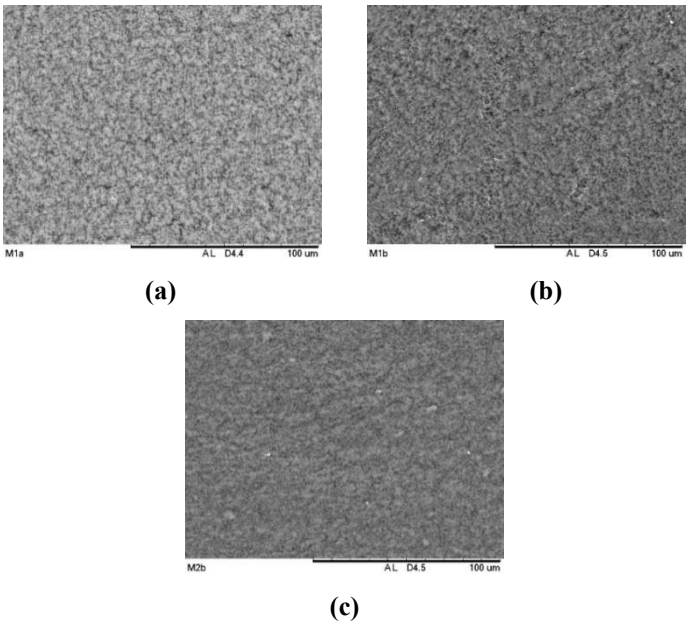

(a) **(b)**

(c)

Fig. 1. SEM images of membrane surfaces (a) M1a, (b) M1b and (c) M2b (1 k ×).

Membranes incorporating MWCNT-PNIPAAm nanocomposites exhibited larger pore size than those containing pristine MWCNTs of the same MWCNTs diameter (M2b: 20.27 nm > M2a: 17.92 nm; M1b: 18.12 nm > M1a: 15.71 nm). This can be attributed to the presence of amide groups (-CONH-) in the PNIPAAm, which increases the hydrophilicity of the nanofillers, thereby increasing the transportation of DMAc and water during the phase inversion process. Consequently, the resulting pores formed are larger in size [13, 16].

Membranes prepared with larger diameter MWCNTs of the same nanofiller exhibit larger pore sizes (M2b: 20.27 nm > M1b: 18.12 nm; M2a: 17.92 nm > M1a: 15.71 nm). This can be attributed to the greater disruption caused by the presence of nanoparticles in the polymer matrix during membrane formation. Larger MWCNTs introduce increased steric hindrance and occupy larger space within the polymer solution. This effect becomes more pronounced when the nanoparticles are not uniformly distributed as it creates regions of stronger polymer disruption. This leads to an overall increase in the average pore size [8, 17]. These trends are qualitatively supported by the cross-sectional SEM images (Fig. 2), where M1b and M2b (Figs. 2(b) and (c) show more interconnected sublayers and enlarged macrovoids compared to M1a (Fig. 2(a)), consistent with the larger pore sizes measured.

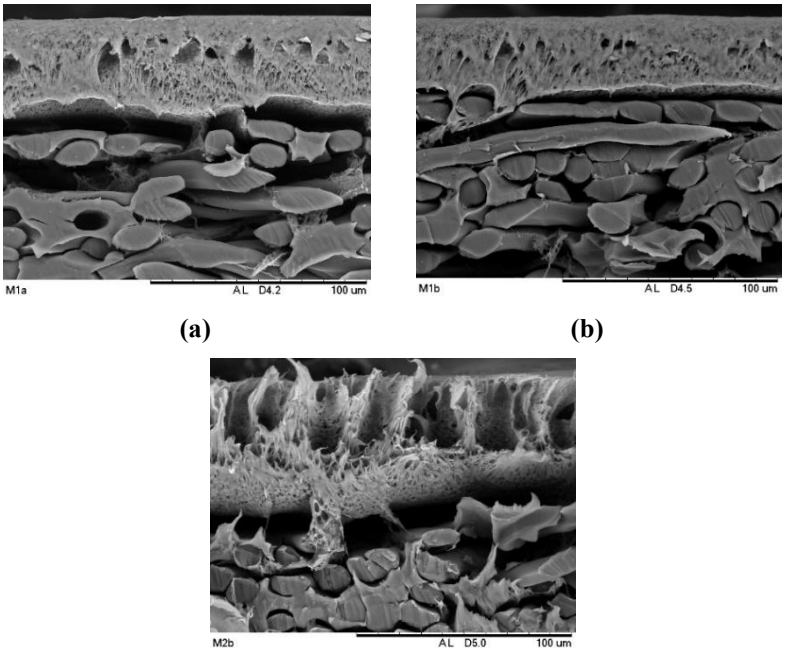

(a) **(b)**

(c)

Fig. 2. SEM images of membrane cross-sections (a) M1a, (b) M1b and (c) M2b (1 k ×).

Table 3 shows the results of the WCA measurements. The incorporation of pristine MWCNTs into the PVDF membrane led to an increase in WCA (M2a: 87.87° > M1a: 87.58° > M0: 71.22°), which indicate increased hydrophobicity. This increase can be attributed to the intrinsic hydrophobicity of pristine MWCNTs, which lack polar groups and possess non-polar graphitic surfaces that repel water molecules [5].

Moreover, the difference in WCA between M1a and M2a is minimal (0.33%), which indicates that increasing the MWCNTs diameter from 12-15 nm to 20-30 nm has little effect. Next, the incorporation of MWCNTs-PNIPAAm into the PVDF membrane resulted in a decrease in WCA (M0: 71.22° > M1b: 71.13° > M2b: 64.14°), which indicates an increase in hydrophilicity. This enhancement is primarily attributed to the presence of -CONH- groups in PNIPAAm. This allows formation of strong hydrogen bonds with water molecules hence increases membrane water affinity [4, 5].

Table 3. WCA of the prepared membranes.

Membrane	Contact angle (°)
M0	71.22 ± 0.91
M1a	87.58 ± 0.09
M1b	71.13 ± 0.91
M2a	87.87 ± 0.26
M2b	64.14± 0.14

3.2. Membrane performance

3.2.1. Membrane permeability

Figure 3 shows the permeability values for all membranes. Overall, permeability increased with the addition of MWCNTs or MWCNT-PNIPAAm nanocomposites, as compared to the unmodified PVDF membrane (M0). Specifically, the permeability of M0 was 18.28 L/m^2·h·bar, which is lower than of the modified membranes (21.90-25.08 L/m^2·h·bar). This trend is supported by porosity and pore size measurements, where the modified membranes showed higher porosity and larger pore sizes compared to M0 (Table 2). Higher porosity and larger pores provide more interconnected pathways, enabling increased passage of water molecules across the membrane [9, 18].

Other than that, hydrophilicity also plays a part in the overall permeability contribution. As mentioned in Table 3. the WCA of M0 was 71.22°, whereas membranes containing MWCNTs-PNIPAAm (M1b and M2b) exhibited lower WCA (64.14 - 71.13°), which indicates a higher hydrophilicity. This allows stronger interaction with water molecules, which facilitates their transport through the polymer matrix [9]. Collectively, the combination structural and surface property improvements result in the enhanced water transport in the modified membranes, while M0 exhibits the lowest permeability.

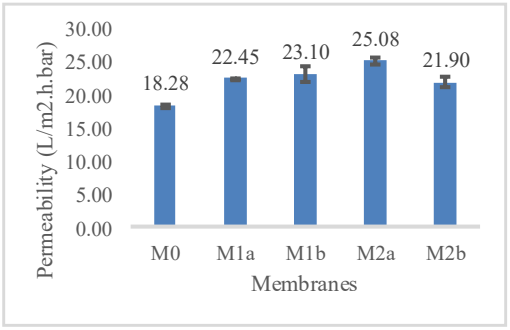

Fig. 3. Water permeability of the prepared membranes.

3.2.2. Normalized flux

Figure 4 shows the normalized flux results for membranes treating SOW. Among the modified membranes, M1b consistently exhibited the highest normalized flux both before (0.579-0.916) and after cleaning (0.663-0.895), whereas M1a showed the lowest (0.410-0.695, 0.406-0.847) under both conditions. Notably, the unmodified PVDF membrane (M0) displayed the second highest normalized flux (0.565-0.878) prior to cleaning but decreased to the lowest normalized flux after cleaning (0.412-0.519) which indicates that the fouling intensified over time. The pronounced decline in post-cleaning flux suggests that the unmodified membrane is more susceptible to colloidal fouling and has reduced cleanability [10].

As shown in Fig. 4, membranes fabricated with MWCNTs-PNIPAAm (M1b, M2b) exhibited higher normalized flux as compared to those fabricated with pristine MWCNTs (M1a, M2a). This is attributed to the introduction of hydrophilic -CONH- groups during PNIPAAm functionalization. In contrast, pristine

MWCNTs reduces membrane hydrophilicity due to their inherently hydrophobic nature [5]. As presented in Table 3, the lower WCA of the MWCNTs-PNIPAAm membranes (M1b = 71.13° and M2b = 64.14°) compared to the pristine MWCNTs membranes (M1a = 87.58° and M2a = 87.87°) promotes water molecule adsorption onto the membrane surface, forming stable hydrated layer that act as barrier to oil particle deposition. This reduces fouling and pore blockage, which allows the membrane to maintain higher normalized flux during filtration [10].

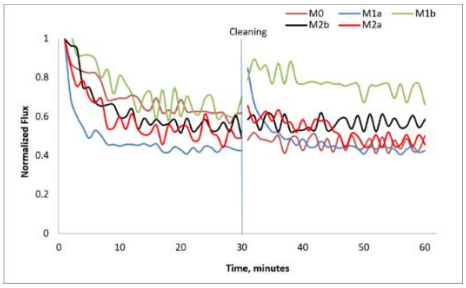

Fig. 4. Normalized flux of the prepared membranes before and after cleaning.

3.2.3. Flux recovery ratio (FRR)

Figure 5 shows the FRR of the prepared membranes. M1b exhibited the highest FRR (0.876), followed by M1a (0.838), M2b (0.740), M2a (0.739) and M0 (0.579), which had the lowest value. The unmodified PVDF membrane (M0) displayed the lowest FRR primarily due to its inherent hydrophobicity, which promotes adhesion of oil particles from the SOW onto the membrane surface. The absence of functionalized nanofillers which can enhance the membrane hydrophilicity means that minimum hydration layer to resist fouling deposition [18]. Membranes fabricated with MWCNTs-PNIPAAm nanocomposites (M1b and M2b) exhibit improved antifouling performance compared to those containing respective pristine MWCNTs with similar diameter (M1a and M2a).

This is due to the integration of the thermoresponsive PNIPAAm polymer into the PVDF polymer matrix which can change between being hydrophilic (-CONH- groups) and hydrophobic ((-$CH(CH_3)_2$) side chains) based on the temperature. At 40 °C, which is above the LCST of approximately 32 °C, the PNIPAAm chains undergo a coil-to-globule transition, exposing hydrophobic groups that help release foulants. Conversely, when cooled to 25 °C, which is below the LCST, the chains adopt an expanded coil structure, increasing hydrophilicity and forming a hydrated layer that resist fouling [4, 5].

This thermoresponsive behaviour supports self-cleaning with only a modest change in temperature. M1b blended with MWCNTs-PNIPAAm with smaller MWCNTs diameter (12-15 nm) exhibited higher FRR (0.876). As compared to M2b blended with MWCNTs-PNIPAAm with larger MWCNTs diameter (20-30 nm), FRR of 0.740 with difference of 16.84%.

This improvement can be attributed to the higher specific surface area and aspect ratio of smaller diameter MWCNTs [19, 20]. This promotes stronger van der Waals interactions with the PVDF matrix. These interactions allow for a more uniform distribution of the MWCNTs-PNIPAAm nanocomposites, with PNIPAAm chains grafted at higher density across the membrane surface. This

ensures consistent formation of the hydrated layer on the membrane surface, enhancing antifouling performance and the thermoresponsive cleaning.

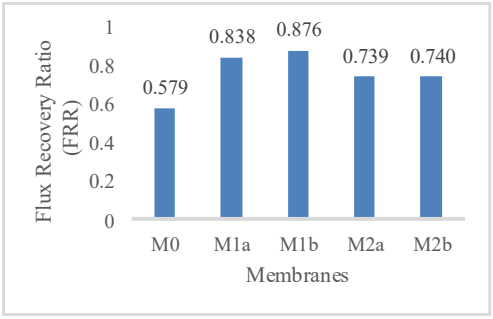

Fig. 5. FRR of the prepared membranes.

3.2.4. Membrane rejection

Figure 6 shows the membrane rejection of all prepared membranes. For the first filtration run (Run 1), the rejection of SOW by the M0 membrane (91.16%) was greater than that of the modified membranes (M1a, M1b, M2a, excluding M2b), which exhibited rejections ranging from 66.65% to 79.32%. This can be explained by the increased porosity and pore size in the modified membranes (Table 2). Hence, the oil particle tends to pass through the membrane easily thereby lower rejection of SOW [10]. Other than that, M2b exhibited the highest rejection (98.82%) in Run 1 compared to all other membranes (66.65 - 91.16%). This greater rejection can be attributed to the greater electrostatic repulsion by -CONH- groups on MWCNTs-PNIPAAm with the negatively charged oil particles [21, 22].

In the second filtration run (Run 2), M0 exhibited the lowest rejection (13.44%), which represents a significant decrease from Run 1 (91.16%) due to its low FRR value (0.579) and residual fouling presented in Fig. 5. Among the fabricated membranes, M2b maintained the highest rejection in Run 2 (85.60%) compared to M1a, M1b and M2a, which exhibited rejections ranging from 68.08% to 80.56%. The slight decrease is likely due to minor residual fouling, while M1a, M1b and M2a remained relatively consistent [23]. Overall, the consistency of rejection in M1a, M1b and M2a across both runs indicates that these membranes maintain stable selectivity and are suitable for long-term operation.

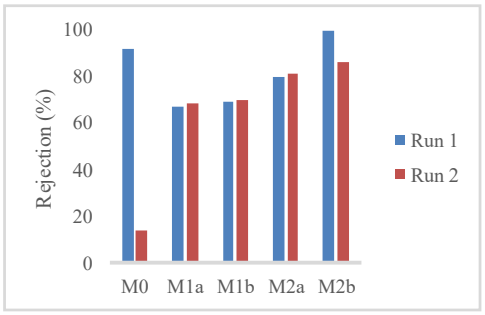

Fig. 6. Membrane rejection of the prepared membranes.

3.3. Membrane Performance for Actual KWW

M1b was selected for evaluation using actual KWW due to the stable and excellent performance during SOW filtration. Table 4 shows the five parameters used for assessment of the quality of the treated water to compare with the NWQSM. COD and TSS removal was high (83.5-84.2% and 83.7-84.4%), reflecting effective removal of organic matter and suspended solids. This can be attributed to the small membrane pore size compared to KWW particles size, which physically blocks these larger particles. TDS removal was low (10.8-23.0%) due to the membrane's ability to retain dissolved species.

Higher removal would require small pore membranes such as nanofiltration or reverse osmosis [10]. Colour decreased substantially (89.3-89.8%), consistent with TSS removal, while pH increased slightly from 6.17 to 7.28. All parameters showed reduction and complied with NWQSM Class IV limits, indicating that the treated KWW has high potential for non-potable reuse, such as irrigation. More parameters such as ammoniacal nitrogen, BOD etc should be investigated in the future to ensure the treated water fully complies the regulation.

Table 4. Measured water quality parameters of actual KWW before and after filtration using the M1b membrane.

Parameter	Initial	Filtration Run		Class IV
		1	2	
COD, mg/L	529.33	83.67	87.33	100
TSS, mg/L	145.33	22.67	23.67	300
TDS, mg/L	74	66	57	4000
pH	6.17	7.28	7.28	5-9
Color, TCU	239.00	25.67	24.33	-

4. Conclusions

This study successfully synthesized the MWCNTs-PNIPAAm thermoresponsive membranes and evaluated for the treatment of KWW. Effect of MWCNTs diameter (12-15 nm, 20-30 nm) were investigated. Incorporation of MWCNTs-PNIPAAm enhanced membrane performance, with M1b blended by MWCNTs-PNIPAAm with smaller diameter of MWCNTs exhibiting high permeability (23.10 $L/m^2 \cdot h \cdot bar$), the highest normalized flux (0.736 before cleaning and 0.774 after cleaning), the highest FRR (0.876) and consistent SOW rejection across two filtration runs (68.45% and 69.30%).

Its superior performance is attributed to a moderate pore size (18.12 nm), high porosity (37.08%) and low WCA (61.4°). During membrane cleaning at 40 °C and 25 °C, MWCNTs-PNIPAAm swelled and shrunk during temperature change providing an effective strong washing force for foulant removal. Besides, the effectiveness in treating actual KWW was demonstrated by its rejection of COD (84.2-83.5%), TSS (84.4-83.7%), TDS (10.8-23.0%), while the colour was reduced by 89.3-89.8% and pH increased slightly from 6.17 to 7.28, with tested parameters complying with the NWQSM Class IV limits, making the membrane suitable for non-potable reuse. These features demonstrate potential of advanced smart

membrane systems with improved efficiency, extended operational lifespan and sustainable wastewater reuse.

Acknowledgements

The authors wish to gratefully acknowledge the financial support by Taylor's University through Taylor's Internal Research Grant Scheme - Impact Lab Grant (TIRGS-ILG) (Project Code: TIRGS-ILG/2/2024/SOE/001).

References

1. Li, W.; Liu, H.; Deng, L.; Zhang, Y.; Ma, Y.; and Chen, Y. (2024). Recent advances in treatment refinement of kitchen digested wastewater: Feasibility, prospects, and technicalities. *Water Cycle*, 5, 20-30.
2. Ahmad, I. et al. (2023). Micro and macro analysis of restaurant wastewater containing fat, oil, grease (FOG): An approach based on prevention, control, and sustainable management. *Chemosphere*, 325, 138236.
3. Daud, Z.; Suhani, N.; Radin Mohamed, R.M.S.; and Awang, H. (2017). Feasibility of banana (*Musa sapientum*) trunk biofibres for treating kitchen wastewater. *Nature Environment and Pollution Technology*, 16(4), 1205-1210.
4. Ngang, H.P.; Ahmad, A.L.; Low, S.C.; and Ooi, B.S. (2017). Preparation of thermoresponsive PVDF/SiO_2–PNIPAM mixed matrix membrane for saline oil emulsion separation and its cleaning efficiency. *Desalination*, 408, 1-12.
5. Yaghoubi, Z.; and Parsa, J.B. (2019). Preparation of thermo-responsive PNIPAAm–MWCNT membranes and evaluation of its antifouling properties in dairy wastewater. *Materials Science and Engineering*: *C*, 103, 109779.
6. Ciarleglio, G.; Toto, E.; and Santonicola, M.G. (2023). Conductive and thermo-responsive composite hydrogels with poly(N-isopropylacrylamide) and carbon nanotubes fabricated by two-step photopolymerization. *Polymers*, 15(4), 1022.
7. Avilés, F.; Sierra-Chi, C.A.; Nistal, A.; May-Pat, A.; Rubio, F.; and Rubio, J. (2013). Influence of silane concentration on the silanization of multiwall carbon nanotubes. *Carbon*, 57, 520-529.
8. Ho, K.C.; Teow, Y.H.; Ang, W.L.; and Mohammad, A.W. (2017). Novel GO/OMWCNTs mixed-matrix membrane with enhanced antifouling property for palm oil mill effluent treatment. *Separation and Purification Technology*, 177, 337-349.
9. Ho, K.C.; Lim, J.H.; Mohd Idris, A.I.; Teow, Y.H.; and Ng, N.C. (2023). Effect of diameter of carbon nanotubes in nanocomposite membrane for methyl orange dye removal. *Journal of Applied Membrane Science & Technology*, 27(1), 47-61.
10. Ho, K.C. (2019). *Graphene oxide/carbon nanotubes conductive membrane with active antifouling properties*. PhD Thesis, Faculty of Engineering and Built Environment, Universiti Kebangsaan Malaysia, Bangi, Malaysia.
11. Department of Environment Malaysia. (2025). National Water Quality Standards. Retrieved May 30, 2025, from https://www.doe.gov.my/en/national-water-quality-standards/

12. Kammakakam, I.; and Lai, Z. (2023). Next-generation ultrafiltration membranes: A review of material design, properties, recent progress, and challenges. *Chemosphere*, 316, 137669.
13. Chen, Y.M.; Ho, K.C.; Chan, M.K.; Teow, Y.H.; Isma, A.; and Idris, M. (2023). Optimization of antifouling properties of mixed matrix membrane synthesized via in-situ colloidal precipitation. *Journal of Membrane Science and Research*, 9(1), 266048401.
14. Sianipar, M.; Kim, S.H.; Khoiruddin, K.; Iskandar, F.; and Wenten, I.G. (2017). Functionalized carbon nanotube (CNT) membrane: Progress and challenges. *RSC Advances*, 7(81), 51175-51198.
15. Xu, T.; Qi, Z.; Tan, Y.; Tian, J.; and Li, X. (2021). Effect of multiwalled carbon nanotube diameter on mechanical behavior and fracture toughness of epoxy nanocomposites. *Materials Research Express*, 8(1), 015014.
16. Mama, L.; Pirkin-Benameur, J.; Bouad, V.; Fournier, D.; Woisel, P.; Lyskawa, J.; Aissou, K.; and Quemener, D. (2025). Development of thermo-responsive and salt-adaptive ultrafiltration membranes functionalized with PNIPAM-co-PDMAC copolymer. *Membranes*, 15(6), 164.
17. Prihandana, G.S.; Sriani, T.; Muthi'ah, A.D.; Machmudah, A.; Mahardika, M.; and Miki, N. (2022). Study effect of nAg particle size on the properties and antibacterial characteristics of polysulfone membranes. *Nanomaterials*, 12(3), 388.
18. Hommel, J.; Coltman, E.; and Class, H. (2018). Porosity-permeability relations for evolving pore space: A review with a focus on (bio-)geochemically altered porous media. *Transport in Porous Media*, 124(2), 589-629.
19. Ghobadi Moghadam, A.; and Hemmati, A. (2023). Improved water purification by PVDF ultrafiltration membrane modified with GO-PVA-NaAlg hydrogel. *Scientific Reports*, 13(1), 8076.
20. Ren, X.; Shi, L.; He, P.; Qian, Y.; Wu, Y.; Zhang, Z.; and Gong, C. (2023). Effects of carboxylated MWCNTs additives on the structure and performance of PMIA membrane: Size, content and PPCPs removal specificity. *Applied Surface Science*, 629, 157454.
21. Karadag, A. (2019). The effects of surfactants on the oxidation of sunflower oil in emulsions. *International Journal of Food Technology and Nutrition*, 2(3-4), 20-24.
22. Hudaib, B.; Abu-Zurayk, R.; Waleed, H.; and Ibrahim, A.A. (2022). Fabrication of a novel PVDF/MWCNT/polypyrrole antifouling high-flux ultrafiltration membrane for crude oil wastewater treatment. *Membranes*, 12(8), 751.
23. Maeda, Y. (2024). Fouling of reverse osmosis (RO) and nanofiltration (NF) membranes by low molecular weight organic compounds (LMWOCs), part 1: Fundamentals and mechanism. *Membranes*, 14(10), 221.